Emergence of Spontaneous Rhythm Disorders in Self-Assembled Networks of Heart Cells

Yoav Soen, Netta Cohen, Doron Lipson, and Erez Braun
Department of Physics, Technion–Israel Institute of Technology, 32000 Haifa, Israel
(Received 3 November 1998)

A noninvasive optical recording technique is introduced to study the spontaneous contractile activity in self-assembled heart cell networks. Continuous monitoring throughout the lifetime of the network reveals spontaneous appearance of various rhythm disorders. Analysis of two typical patterns, namely, subharmonic structures and sudden alternations between two dominant rates, indicates the emergence of intrinsic pacemakers. A model of one or two slightly variable nonlinear oscillators, acting on an excitable element, is shown to reproduce the main experimental results. [S0031-9007(99)08934-6]

PACS numbers: 87.17.Nn, 05.45.Xt, 87.19.Ff

Cultured networks of heart cells serve as a model system for biological networks with strong nearest-neighbor coupling. Studies of *externally* stimulated cardiac preparations have revealed various forms of complex dynamics reflecting the nonlinear nature of those systems [1]. Other studies were aimed at understanding the short-term process of synchronization between periodically beating centers of activity [2]. In both cases, the spontaneous behavior was assumed to be simple (either quiescent or regular rhythmic behavior) and therefore ignored. A hint that the background activity might be more complex was given in a recent work [3], which reported the spontaneous initiation and termination of large-scale spiral waves in cardiac networks. However, the long-term dynamics on small (sub-mm) scales and the relation between synchronization and regularity in such networks have not been investigated.

Here, we study the spontaneous spatiotemporal contractile activity during the process of network self-assembly. We find complex temporal dynamics over a wide range of time scales and focus on two typical dynamical patterns: (I) Subharmonic modes with irregular intermode transitions, and (II) sudden alternations between two rates (intermittent dynamics). Spatiotemporal correlation analysis reveals a high degree of synchronization, regardless of the temporal dynamics. In addition, the data indicate the development of one or more independent and relatively stable (over many hours) pacemakers. We therefore propose a model of one or two pacemakers, driving an excitable medium, which accounts for these rhythm disorders.

Experiments were performed on cultures of spontaneously beating ventricular cells [4]. Isolated cells were plated at the desired density on collagen-coated glass Petri dishes and cultured on an inverted microscope stage (Zeiss Axiovert 135) under sterile incubating conditions (37 °C, 6% CO_2, and on-stage feeding). Following plating, the cells migrate, proliferate, and gradually form a confluent monolayer of cells. At a later stage (usually within 2 weeks), a spontaneous transition to a fibrous morphology usually occurs. Here, we concentrate on moderately dense cultures that form an extended network of cells, in either the monolayer or fiber morphology.

To study the spontaneous dynamics throughout the self-assembly process, a method of continuous, noninvasive, and high-resolution measurement is introduced. The optical field is captured by a charge-coupled device camera and transmitted to a computer, where real-time motion detection is performed. Local contraction traces are obtained by frame-to-frame subtraction of light intensity over prespecified areas of interest. Spike profiles (ranging over 150–300 msec) are clearly resolved with 40 msec video sampling intervals. Off-line peak detection yields a time series of interspike intervals (ISIs). In this way, contractions of single cells as well as networks are recorded at high spatial resolution for durations limited, in practice, only by the lifetime of the culture (typically 3–4 weeks). Later confirmation of the activity and its correlation with morphological changes are performed by samples of real-time and continuous time-lapse video recordings.

Network behavior often consists of periodic beating that is synchronized throughout the field of view (up to 2.5 mm). However, sufficiently long recordings reveal complex rhythm disorders. Figure 1 presents the history of activity in a typical developing network that is monitored continuously for 11 days. This period spans the monolayer and the fibrous phases, separated by approximately two days with no beating (between Figs. 1c and 1d). Figure 1a shows the ISI trace recorded from one area of the network during the early stages of synchronized activity (the first 21.5 h). A phase of monoperiodic beating with a gradual drift towards slower rates is followed by a long interval of irregular beating, which evolves into a pattern of intermittent bursts of irregular and regular beating (in one of two possible modes). This pattern persists throughout most of Fig. 1b. Further network development results in a gradual decay of the intermittent pattern into 53 h of monoperiodic activity (Figs. 1b and 1c). Then, following two days with no beating, a morphological transition from a monolayer into a fiber led to an immediate resumption of activity. Figure 1d shows the ISI trace during this transition and thereafter (70 h).

 0031-9007/99/82(17)/3556(4)$15.00

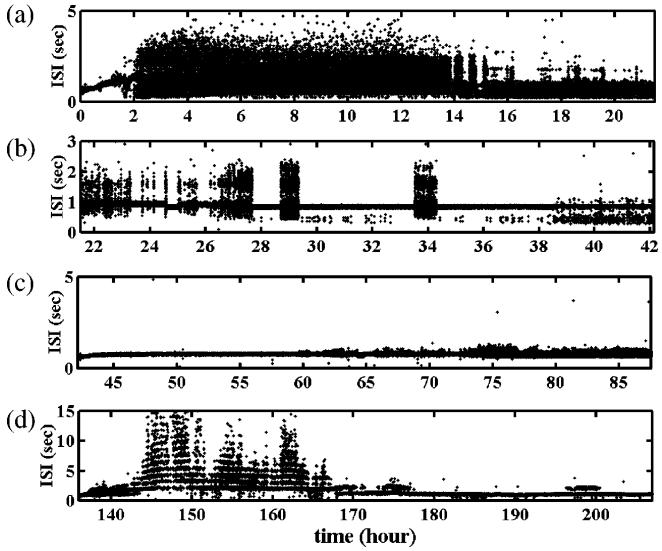

FIG. 1. ISI dynamics during network development. (a) The first 21 h, exhibiting drifting monoperiodic beating, irregular activity, and intermittent bursts of irregular beating. (b) The continuation of the intermittent pattern, leading to hours of monoperiodic beating (c). (d) The buildup and decay of subharmonic structures. A gap of ~48 h between (c) and (d) is due to a silent period. Note the differences in vertical scales.

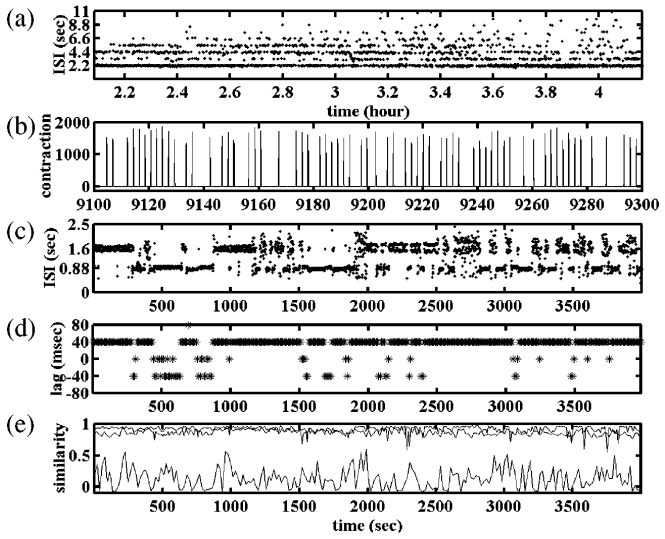

FIG. 2. (a) A 2-h portion of the subharmonic ISI trace of Fig. 1d. (b) A contraction trace for part of (a). (c) The inner structure of one of the bursts of Fig. 1b, revealing irregular transitions between two beating periods (0.88 and 1.6 sec), and occasional bursts of less regular beating. (d) A dynamic time-lag trace, computed for the interval in (c). Note the coincidence between time lags and rate alternations. (e) Similarity traces in the intermittent and subharmonic patterns (upper two traces), as compared with that of the same region at different time intervals (lower trace).

It reveals a dynamical process of progressive buildup and decay of integral multiples of a fundamental period (or frequency subharmonics). Interestingly, the fundamental mode is absent during most of this time. All these patterns are commonly observed in our cultures, yet their specific combination and order do not form a general description of network development. Figure 2a shows a 2-h portion of the subharmonic pattern of Fig. 1d, consisting of exact subharmonics of an absent ($\overline{\mathrm{ISI}} = 1.09$ sec) fundamental mode. The subharmonic distribution is modulated on time scales, ranging from seconds to hours, yet the fundamental mode is insensitive to these modulations. Typical contraction traces (Fig. 2b) include period-two (i.e., beating at half the fundamental frequency) and occasional period-three repeating sequences that are separated by bunches of higher-period intervals. More complex repeating sequences seldom appear.

While the entire field of view appears to beat synchronously (exhibiting homogeneous dynamical patterns), small time lags can be detected between different areas. In order to better estimate these time lags and to examine the relation between the temporal patterns and the degree of synchronization, a similarity function is derived as follows. Given a pair of amplitude traces $f_1(t)$ and $f_2(t)$ from two different areas, traces of local correlation coefficients $S_\tau(t)$ are computed between the first trace and a second locally time-shifted trace (locality is obtained by dividing time into bins of few seconds length).

$$S_\tau(t) = \frac{\mathrm{cov}[f_1(t), \xi f_2(t - \tau(t))]}{\sqrt{\mathrm{var}[f_1(t)]\ \mathrm{var}[\xi f_2(t - \tau(t))]}},$$

where $\tau(t)$ is the trace of local time shifts and ξ is a global normalization parameter obeying $\mathrm{mean}[\xi f_2(t)] = \mathrm{mean}[f_1(t)]$. The similarity function $\overline{S}(t)$ is defined as the trace $S_\tau(t)$ for which $\tau(t)$ locally maximizes the correlation coefficients, and the optimal trace of time shifts is defined as the time-lag trace $\overline{\tau}(t)$ between the corresponding regions. When $\overline{\tau}(t)$ is dynamic, the time shifts $\tau(t)$ must be bound to a small fraction of the mean ISI, to avoid compensating low correlation by large time shifts. Thus, for uncorrelated signals $\overline{S}(t)$ is low, whereas for synchronized or slightly (and locally) shifted signals, $\overline{S}(t) \to 1$. Figure 2e shows typical $\overline{S}(t)$ traces for both uncorrelated and correlated signals. The lower trace is obtained for the same region at different times, whereas the two upper traces are computed for different regions at the same time. One of the upper traces is computed for the two farthest regions (about 2.3 mm apart) during the subharmonic interval of Fig. 2a. For this interval, $\overline{\tau}(t)$ between any pair of regions is constant in time, but increases linearly with the distance along the fiber, indicating a propagation velocity of about 10 mm/sec (about an order of magnitude smaller than values reported for very dense cultures [5]).

We turn now to the intermittent pattern of Fig. 1b. A 66 min portion of it is shown in Fig. 2c. The trace includes irregular transitions among three modes of activity: a fast rate (with a period ~0.88 sec), a slow rate (~1.6 sec), and a less regular mode. The typical time

scale of these rate alternations is a few tens of seconds. Here, by contrast to the subharmonic pattern, $\overline{\tau}(t)$ is dynamic, and reveals (Fig. 2d) an interesting correlation between rate and time-lag alternations: The slower rate and the less regular beating usually coincide with positive time lags, whereas sufficiently long stretches of faster activity coincide with zero or negative time lags. Examination of time lags between all the regions associates the rate alternations with corresponding alternations in the direction of propagation. Finally, the high degree of similarity for both the subharmonic and the intermittent patterns (upper traces of Fig. 2e) points to the insensitivity of spatial correlations to changes in the temporal dynamics.

Thus, both dynamical patterns exhibit propagation effects and complex temporal dynamics, characterized by one or two stable frequencies, suggesting the emergence of one or more pacemakers, which provide stable and fixed stimuli to the rest of the network. In the subharmonic case, the skipped beat structure and the linearly increasing time lags indicate a unidirectional coupling of the network to a single, fast pacemaker, which interferes with the recovery mechanism of the excitable medium and leads to reduced excitability and loss of 1:1 phase locking. The higher the stimulation frequency, the lower the ratio of responses m to stimuli n. The absence of the fundamental frequency is a strong signature of an n:m entrainment by a fast pacemaker. The intermittent pattern, which exhibits two frequencies with alternating time lags, seems more complicated, and suggests two opposite fronts, propagating from two independent pacemakers. To reproduce the key features of both patterns, we propose a model comprising one or two nonlinear oscillators driving an otherwise quiescent excitable element. Each component (oscillator or excitable medium) is represented by Morris Lecar equations [6], with two dynamic variables v and w, that may be interpreted as the membrane potential and the fraction of open ion channels of a single type, respectively. (This model is chosen only for convenience, as the main results are model independent.) The dynamic variables evolve according to two dimensionless first order differential equations:

$$\frac{dv}{dt} = -\overline{g}_{Ca}\, m_\infty(v)\,(v - 1) - \overline{g}_K w (v - v_K) - \overline{g}_L (v - v_L) + I_{\text{ext}} + I_{\text{coup}}\,,$$

$$\frac{dw}{dt} = \phi\,\frac{[w_\infty(v) - w]}{\tau_w(v)}\,,$$

where ϕ is a rate parameter, $\overline{g}_{Cai}, \overline{g}_K, \overline{g}_L$, v_K, and v_L represent different conductances and reversal potentials, and m_∞, w_∞, and τ_w are functions of v (given in [6]). The classification of a component as a pacemaker or a quiescent element is determined by I_{ext}. The coupling term $I_{\text{coup}} = \sum_j K_j(v_j - v)$, comprising a sum of independent Ohmic currents $K_j(v_j - v)$, appears only in the equation for the excitable element.

The subharmonic pattern is modeled by an excitable element, coupled unidirectionally to a single pacemaker, with a slightly noisy rate. Numerical simulations show that the coupling K acts as a bifurcation parameter between different n:m patterns [7]. For a noiseless pacemaker and large enough K, the excitable element is 1:1 phase locked. With the reduction of K, two (decreasing) period-adding sequences appear: first an $(n + 1)$:n sequence, in which every n beats are followed by a skipped beat, and then a $(2n + 1)$:n sequence, in which every $2n$ beats are followed by a skipped beat [8]. Both sequences satisfy the universal scaling law of $[K_{(\infty)} - K_{(n)}] \propto n^{-2}$ [9]. Below some threshold value $K < K_{\text{th}}$, the response of the excitable element is passive. In the vicinity of this threshold, small rate variability of the pacemaker (or alternatively, small coupling variations) induces transitions among subharmonics. In particular, random rate changes result in an irregular subharmonic pattern. Figure 3a shows a typical pattern, generated by this model [10]. In this example, K is just over the threshold, and rate variability is introduced by adding white noise to the pacemaker's rate parameter ϕ. The noise amplitude is chosen to yield lower rate variability than in our most regular recordings [std(ISI)/mean(ISI) $\sim$ 0.04; std: standard deviation]. Similar to the data, deviations from a period-two pattern occur irregularly (Fig. 3b) but are positively correlated, and the abundance of subharmonic modes is nonexponential.

The intermittent pattern is modeled by including an additional pacemaker, with a slightly different (not

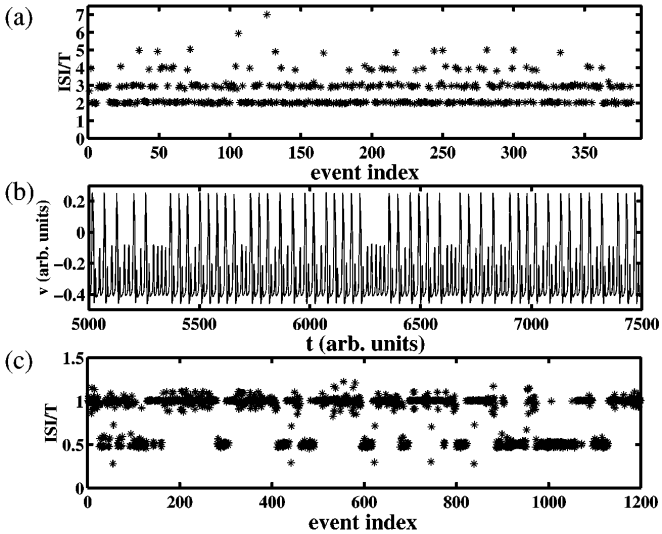

FIG. 3. Typical model results. (a) A subharmonic trace of ISIs (divided by the excitation period T) of an excitable Morris Lecar element driven by a single pacemaker. (b) A portion of the raw trace revealing (2:1) sequences that are often separated by higher-period ISIs. (c) An intermittent ISI trace of an excitable element driven by two independent pacemakers.

necessarily variable) frequency. Here, by contrast to the subharmonic pattern, an interference with the recovery is not necessary, so that the pacemakers' rate may be relatively low. Figure 3c shows a typical ISI trace obtained by a simulation of two pacemakers, with a 1% frequency difference Δf [10]. The resulting dynamics include irregular transitions between a slow rate and its (approximately) first multiple. These transitions can be understood as a simple interference effect: A small Δf induces a periodic phase difference $\Delta\varphi$ (with a period inversely proportional to Δf). When $\Delta\varphi$ is small, the excitations interfere constructively, so that the excitable element is entrained, in a 1:1 manner, to an excitation profile with one peak per period. As $\Delta\varphi$ increases, the combined excitation profile becomes double-peaked, resulting in a (still) 1:1 entrainment to an approximately doubled effective excitation frequency. The addition of a small noise term into the rate ϕ of one of the pacemakers leads to random phase resetting of its period and eliminates the periodicity of rate alternations.

In summary, long-term recordings of spontaneous contractile activity of cultured networks of heart cells reveal complex deviations from rhythmic behavior, spanning a wide range of time scales. The analysis of two typical deviations suggests that, in contrast to a naive view of symmetrical coupling among a homogeneous population of nonlinear oscillators, the network differentiates inhomogeneously into a hierarchy of components, comprising pacemakers, excitable media, and asymmetric conduction paths. This picture is supported by the above model that associates the appearance and long-term modulation of the temporal patterns with coupling dynamics. Further work along the line presented here will provide more insight into the development of activity and functionality in biological networks.

We thank L. Glass, S. Marom, and S. Lipson for valuable discussions. This work has been supported by the U.S.–Israel Binational Science Foundation, Grant No. 94-262.

[1] M. R. Guevara, L. Glass, and A. Shrier, Science **214**, 1350 (1981); D. R. Chialvo and J. Jalife, Nature (London) **330**, 749 (1987).

[2] D. L. Ypey, D. E. Clapham, and R. L. DeHaan, Mem. Biol. **51**, 75 (1979); J. Jalife, J. Physiol. **356**, 221 (1984).

[3] G. Bub, L. Glass, N. G. Publicover, and A. Shrier, Proc. Natl. Acad. Sci. U.S.A. **95**, 10 283 (1998).

[4] Ventricles are excised from day-old rats, rinsed in saline solution (PBS with 1M D-glucose and 1% penicillin-streptomycin), minced into pieces, and mixed in RDB solution (saline solution with 1% RDB cutting enzyme, Israel Inst. for Biol. Res., Nes Ziona, Israel). The solution is stirred for 10-min intervals (approximately 15 times). Following each stirring period the supernatant is removed and centrifuged with additional growth medium (F10 [Ham] with L-glutamine, 5% HS, 5% FCS, 1% penicillin-streptomycin, 1 mM $CaCl_2$). The cells are then recombined, filtered, centrifuged again, and diluted in growth medium to the desired density. Medium is changed one day after plating and every 2–3 days thereafter.

[5] V. G. Fast and G. Kleber, Circ. Res. **75**, 591 (1994).

[6] J. Rinzel and G. B. Ermentrout, in *Methods in Neuronal Modeling*, edited by C. Koch and I. Segev (MIT Press, Cambridge, MA, 1989).

[7] Numerical integration is performed by MATLAB's ODE45 solver at relative and absolute tolerances of 1×10^{-7} and 1×10^{-9}, respectively. The results were verified qualitatively with the ODE15 stiff solver.

[8] N. Takahashi, Y. Hanyu, T. Musha, R. Kubo, and G. Matsumoto, Physica (Amsterdam) **43D**, 318 (1990).

[9] K. Kaneko, Prog. Theor. Phys. **68**, 669 (1982).

[10] Subharmonic model parameters (first number corresponds to the pacemaker): $I = (0.1, -0.1)$; $\overline{g}_{Ca} = (1, 1.4)$, $\overline{g}_K = (2, 2)$, $\overline{g}_L = (0.556, 0.51)$, $\phi = (1, 0.078)$, $v_k = -(0.7, 0.7, 0.7)$, $K = 0.7498$, and noise std $= 0.0025$. Intermittent model parameters (first two numbers correspond to the pacemakers): $\overline{g}_{Ca} = (1, 1, 1.4)$, $\overline{g}_K = (2, 2, 2)$, $\overline{g}_L = (0.5, 0.5, 0.33)$, $\phi = (0.2, 0.195, 0.07)$, $v_k = (0.7, 0.7, 0.62)$, $K_1 = K_2 = 1$, and noise std $= 0.0055$. In all cases, $v_l = -0.5$, and the parameters of the functions m_∞, w_∞, and τ_w (given in [6]) are $v_1 = -0.01$, $v_2 = 0.15$, $v_3 = 0.1$, and $v_4 = 0.145$.